

Received June 25, 2020, accepted July 26, 2020, date of publication August 11, 2020, date of current version August 24, 2020.

Digital Object Identifier 10.1109/ACCESS.2020.3015761

# Toward Universal Neural Interfaces for Daily Use: Decoding the Neural Drive to Muscles Generalises Highly Accurate Finger Task Identification Across Humans

MARTYNA STACHACZYK<sup>1</sup>, (Graduate Student Member, IEEE),  
S. FAROKH ATASHZAR<sup>2</sup>, (Member, IEEE), SIGRID DUPAN<sup>3</sup>, (Member, IEEE),  
IVAN VUJAKLIJA<sup>4</sup>, (Member, IEEE), AND DARIO FARINA<sup>1</sup>, (Fellow, IEEE)

<sup>1</sup>Department of Bioengineering, Imperial College London, London SW7 2AZ, U.K.

<sup>2</sup>Tandon School of Engineering, New York University, New York, NY 11201, USA

<sup>3</sup>School of Engineering, Newcastle University, Newcastle upon Tyne NE1 7RU, U.K.

<sup>4</sup>Department of Electrical Engineering and Automation, Aalto University, 02150 Espoo, Finland

Corresponding author: Dario Farina (d.farina@imperial.ac.uk)

This work was supported in part by the European Research Council Synergy project Natural BionicS under Grant 810346, and in part by the U.K. Engineering and Physical Sciences Research Council (EPSRC) under Grant 197594.

**ABSTRACT** Peripheral neural signals can be used to estimate movement-specific muscle activation patterns for the purpose of human-machine interfacing (HMI). The available HMI solutions, however, provide limited movement decoding accuracy that often results in inadequate device control, especially in the dynamic tasks context, and require extensive algorithm training that is highly subject-specific. Here, we show that dexterous movements can be identified with high accuracy using a physiology-derived and information-theoretically optimised feature space that targets the spatio-temporal properties of the spiking activity of spinal motor neurons (neural features), decomposed from the interference myoelectric signal. Moreover, we show that the movement decoding accuracy based on these neural features is not influenced by the muscle activation level, reaching overall >98% in the full range of forces investigated and from processing intervals as short as 30-ms. Finally, we show that the high accuracy in individual finger movement recognition can be achieved without user-specific models. These results are the first to show a highly accurate discrimination of dexterous movement tasks in a wide range of muscle activation levels from near-real time processing intervals, with minimal subject-specific training, and thus are promising for the translation of HMI to daily use.

**INDEX TERMS** Dexterous movement classification, human-machine interfaces, information theory, neural drive, universality of neural control.

## I. INTRODUCTION

A fundamental role of the human nervous system is to generate goal-oriented behaviour. Behaviour, such as walking, eye-gazing or grasping, is expressed in the form of a controlled movement [1], [2]. In times of a rapid development of human-machine interfaces (HMIs) and common access to smart devices, considerable efforts are being made towards identifying neural correlates of movement intention [3]–[6] and movement execution [6]–[8]. The decoding of basic kinetic [9] and semantic [10] movement components, such

as the amount of force exerted by a muscle or the actuation of a specific degree of freedom (DOF), is at the core of HMIs, with applications for healthy users as well as patients with motor impairments. Movement-decoding paradigms have the potential to replace the currently available, indirect interfacing that makes use of a ‘medium’ device, such as a switch or a keyboard, in order to perform an operation, and introduce direct machine control, with which the user can operate a device using different features and levels of muscle excitation [11]–[13]. The direct interfacing not only can change the way we use smart devices recreationally, but it can also bring numerous clinical perks, such as novel rehabilitation strategies and improved neuroprosthetic control.

The associate editor coordinating the review of this manuscript and approving it for publication was Hasan S. Mir.

However, fulfilling the demand for deconstructing the movement into its basic spatio-temporal components remains challenging [14]–[17]. Some attempts for non-invasive HMIs rely on electroencephalographic signals (EEG) recorded from the central nervous system (CNS) for translating the movement intention into commands to external devices [14], [18], [19]. These solutions provide insufficient spatio-temporal resolution of movement correlates, and thus yield limited accuracy and robustness. The CNS coordinates voluntary movements through the activity of spinal motor neurons that innervate the muscle tissue which, when excited, contracts to generate force [20]. An approach alternative to EEG for neural decoding of movements is thus based on peripheral decoding via the identification of the behaviour of spinal motor neurons [21]. Decoding can be achieved with the decomposition of non-invasive, high-density EMG signals (HD-EMG) [22], [23]. HD-EMG, which record muscles' activity from several closely spaced electrodes over the skin, can be decomposed into motor unit action potentials that correspond to the discharge timings of the innervating motor neurons (i.e., the neural drive to the muscle) [24]. The decomposition can be performed with online implementations and therefore is suitable for HMIs [25], [26]. While motor neuron discharge timings have been previously exploited for movement recognition purposes in classic machine learning paradigms [21], [27]–[29], there have been no attempts to extract physiology-inspired characteristics from decoded motor neuron behaviour to estimate user motion. By investigating the physiological features leading to the movement generation, we aim to obtain a truly robust direct interfacing that could substantially increase the translational potential of movement decoding methods. In this paper, we extract features from decoded motor neuron behaviour that physiologically explain force generation as a combination of recruitment and rate coding of motor units [30], [31]. We present accurate tracking of movement phases in finger control, based on information on the behaviour of motor neurons identified from the decomposed HD-EMG signal. Moreover, we propose that this neural information conveys universal movement execution code in humans, so that the identification of movement from peripheral neural correlates is possible without user-specific models. By demonstrating that a fully non-invasive derivation of neural correlates of movement is feasible and demonstrating the proof of concept of the peripheral neural control universality in humans, we provide a significant step forward towards a better integration of HMI systems in our daily living.

## II. METHODS

### A. DATA ACQUISITION

The experiments were conducted on nine able-bodied, right-handed participants (age  $26.5 \pm 2.4$  years, 4 males and 5 females). All participants were naive to the experimental setup. The experimental protocols as well as the informed consent forms for the experiment were

approved by the Imperial College London Research Ethics Committee. Myoelectric signals were recorded from the flexor digitorum superficialis muscle (FDS) with an HD-EMG electrode system of 64 sensors during individual flexions of the index, middle, ring and little finger. The EMG signals were amplified with a gain of 500-1000 (OT Bioelettronica EMG-USB2), band-pass filtered at 10-500 Hz, sampled at 2048 Hz, and transmitted to the host PC. The participants were seated in front of a computer screen with their wrist stable and digits rested on top of individual force sensors (Phidgets Inc, Calgary, Canada). Visual cues were presented on a computer screen to indicate which digit to activate. Finger flexions were performed in a ramp mode, comprising four movement phases: resting (REST), force increase (ASC) (2 s), stable force at 25% Maximum Voluntary Contraction (MVC) (PLAT) (5 s), and force decrease (DESC) (2 s). The setup and data collection lasted for 45 minutes and consisted of three repetitions of individual finger presses performed in randomized order.

### B. HD-EMG DECOMPOSITION

The HD-EMG signals were resolved into series of discharge timings of active motor neurons following the Convolution Kernel Compensation (CKC) method [32]. The CKC algorithm is based on a convolutive data model of surface myoelectric signals in which the multi-channel EMG signal is convolved in the spatio-temporal domain by estimates of separation vectors for individual motor units. Activity of motor neurons is modelled by series of discrete delta functions that correspond to their respective discharge times. The CKC approach was chosen since it is proved to assure a good approximation of complete Motor Unit (MU) discharge patterns during low-level force-varying contractions. The decomposition results were held to the standards of signal-based metrics of accuracy – the pulse-to-noise ratio (PNR), assuring that only the MUs decomposed with  $\text{PNR} > 30\text{dB}$  were analysed.

### C. FEATURE SPACE

To describe the global myoelectric activity, we calculated the Root Mean Square (RMS) of each channel of the HD-EMG recording. RMS is an estimator of EMG amplitude and provides information on the muscle activation level. To characterise the neural activity, we estimated pooled motor neuron spike trains based on the number of spikes (spike count – SC), the standard deviation of the times of motor neuron discharges (STD), and the average inter-spike-interval (ISI) measures. This set of variables targeted both peripheral and central properties of the active motor units, with SC being directly proportional to the force exerted by the muscle during a contraction, and STD and ISI representing spike train metrics that quantify the temporal and topological similarities and dissimilarities of all-or-none neural cortical events [33]. The feature space was participant-specific and contained information from  $n$  EMG sensors that measured the muscle activity over the time interval  $T$ .  $T$  was processed in uni-

form  $k$ -size windows. In this paper, the size of  $k$  was set to 30-ms (or 30- and 150-ms, respectively, for two-conditional interference EMG signal processing), representing a trade-off between the real-time processing of myoelectric signals and an accurate phase-and-DOF discrimination. The final structure of the feature matrix was three-dimensional ( $n \times m \times l$ ), comprising  $n$  rows corresponding to EMG electrodes ( $n = 64$ ),  $m$  columns corresponding to the processing windows (where  $m = \frac{T}{k}$ ), and the  $l^{\text{th}}$  dimension representing different feature types (i.e. SC, STD and ISI for the neural input ( $l = 3$ ), and RMS for the interference EMG ( $l = 1$ )). To enhance the spatial selectivity of the feature space, we ranked all individual electrodes based on their average RMS score. Following ranking, an activation threshold was imposed on the electrode space which allowed for retaining the features characterising the signals that scored  $\geq 70\%$  of the maximum average RMS value. The electrodes that did not meet the activation thresholding condition were set to zero in the feature space.

#### D. MUTUAL INFORMATION FOR THE FEATURE SPACE OPTIMISATION

To decrease the redundancy within the neural feature space, we applied the Information Theory's Mutual Information (MI) measure to compute the entropies of individual features as well as the joint MI between features [34]. The MI between each of the random variables was estimated by binning (bin size being equal to processing window) that allowed for the approximation of their probability density functions. Next, the MI was calculated according to the following equation:

$$I(s; r) = \sum_s \sum_r p(s, r) \log_2 \frac{p(s, r)}{p(s)p(r)} \quad (1)$$

where  $s$  and  $r$  are discrete random variables,  $I(s; r)$  is the MI between them, and the summations are calculated over the appropriately discretized values of the  $s$  and  $r$ . For each bin, the joint probability distribution  $p(s, r)$  was estimated by counting the number of cases that fell into a particular bin and dividing that number with the total number of cases. The same technique was applied for the approximation of the marginal distributions  $p(s)$  and  $p(r)$ .

#### E. CLASSIFICATION

We used two types of classification inputs and three types of classification tasks. In the first classification task we tested the capacity of using peripheral signals for effective movement tracking (i.e. muscle contraction stages discrimination) of a single-DOF activation. In the second task, which constituted an extension of the results obtained with the first task, we tested whether the information contained in peripheral signals allowed for effective movement tracking concurrently with the accurate differentiation between different DOFs. In the third task, we assessed the classification of DOFs activation only by pooling all force levels. To compare the accuracy achieved with the conventional, global HD-EMG

approach and that of the proposed neural approach for movement decoding, we performed a comparative analysis on the respective types of input in the first and the third discriminative tasks. We excluded the interference EMG analysis in the second classification task based on the very poor performance of this approach in the first task, which was a less complex version of the second task.

#### F. PERFORMANCE ASSESSMENT

To test and compare performances of global and neural discriminative approaches, a classification into discrete classes (i.e. fingers' movements and/or phases of fingers' movements) was performed using a linear discriminant analysis (LDA) [35] with Monte-Carlo cross-validation (MCCV) [36], [37]. In a dataset of  $n$  instances, an MCCV procedure randomly generated without replacement  $k$  subsets, each of which contained  $m$  instances, where  $n = k \times m$ . In each iteration, a different  $k$  subset is held out to estimate the classification error while the remaining  $k - 1$  subsets are used for training. A fixed 5:1 train-test ratio was kept throughout the conducted discriminative performance analysis.

To examine the universality of the peripheral information, we performed a classification into the discrete classes using LDA with one out of two variants of a leave-one-subject-out cross-validation (LOOCV) [38], [39]. In classic LOOCV, a single observation corresponds to an individual participant's dataset which is used as classification validation set. In the complete LOOCV variant, called LOOCV (1), we used a single observation as the validation set and the remaining observations (8) as the training set. In the incomplete LOOCV variant, called LOOCV (2), we randomly selected without replacement 5% of a single-observation validation set and included it in the training set along the remaining observations. This introduced a small amount of 'same-source' observation to the classifier's training that could increase the classification accuracy due to sharing of the feature space's pattern with the validation set.

#### G. STATISTICAL ANALYSIS

Normality of the data was assessed by the Shapiro-Wilk test. When the null hypothesis of skewed distribution was rejected, the independent samples t-test was used for determining whether samples in different groups (e.g., different DOFs) originated from the same distribution. When this null hypothesis was rejected, post-hoc pair-wise comparisons were performed with the Wilcoxon signed. Post-hoc analysis was performed with the Tukey test. The threshold for significance throughout the analysis was set to  $p < 0.05$ .

### III. RESULTS

#### A. DECODING MOVEMENT PHASES

Decoding the peripheral correlates of volitional movements requires identifying the fundamental spatio-temporal components of the neural activation to muscles. For this purpose, muscles' electrical activity can be decomposed into

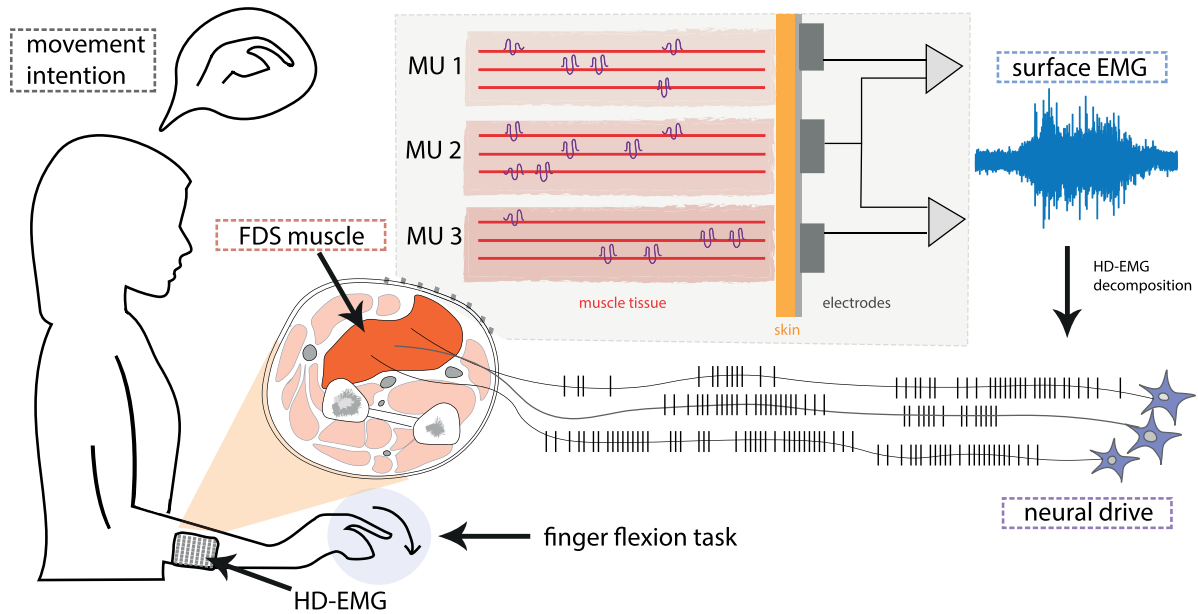


**FIGURE 1.** Intended movement generation and signal decomposition. The movement intention triggers the motor neuron activity (i.e. the neural drive to the muscle), exciting the muscle fascicles. The change in muscle fascicles' length influences the recruitment and discharge rate of motor units (MUs), allowing for a proportional actuation of the intended DOF. The myoelectric signal elicited within the muscle during DOF actuation is acquired using a high-density electrode grid placed on the skin overlaying the active muscle, resulting in the EMG recording. The HD-EMG signal can be then decomposed into neural drive that corresponds to a particular movement.

the neural drive down-streamed from the spinal cord via motor neurons. We explored the feasibility of distinguishing movements (DOFs) during their contraction stages (increase/decrease/stable force) based on motor neuron activity decoded from myoelectric signals (Fig.1). The number of spikes and sparseness of the spike trains vary as a function of MU recruitment and rate coding, which are the two physiological mechanisms that determine force modulation. Moreover, each identified MU can be characterised by its spatial location, as estimated by the amplitude distribution of its MU action potential recorded with the HD-EMG grid (see Supplementary Fig. 3). We calculated an averaged RMS value on spike trains in order to score the activation level of each HD-EMG electrode, and then set an activation threshold on the electrode space so that only the signals from the electrodes overlying the most active compartments of the FDS muscle were included in the feature space for each contraction. We then compared the discriminative capacity of global EMG features (conventional myocontrol) vs MU-based features in different phase-and-DOF classification tasks. To keep the dimensionality of the two classification inputs consistent, we applied the activation thresholding on the electrodes when constructing both neural and global HD-EMG feature spaces for all the classification tasks. Since the neural drive was described by several features (see Methods section), we calculated the mutual information (MI) and Poisson probability density function (PDF) to minimise redundancy of the neural feature space (see Methods section). In Fig. 2a-b (as well as in Appendix, Supplementary Fig. 2.) we show that the features extracted from the neural drive to the muscle were

complementary in both movement phase-and-DOF characterisation contexts.

The feature extraction for the neural input was conducted in 30-ms processing windows, introducing a small delay with respect to processing the signals in real-time. As a comparison, current HMIs used for control of rehabilitation devices, such as prostheses, usually work on intervals of 200-ms. Since the behaviour of MUs changes as a function of the contraction force and of the direction in force modulation, the extracted neural input allowed for tracking the movement phases with high accuracy (Fig. 3a;  $\bar{x}$  97%,  $+/-$  2.81, *specificity* = 97.9%, *sensitivity* = 98.9%). This result demonstrates that the proposed neural features characterised the motor tasks in their specific qualities as to capture differences that are indistinguishable when assessing the global EMG.

To characterise the HD-EMG signal, we applied the electrode thresholding and extracted the RMS from the signals obtained from the most active FDS compartments. The RMS extraction for the global input was conducted in 30-ms (for comparison with neural features) and 150-ms (considering the optimal window duration for EMG-based classification of movement phases [42]) intervals. The global EMG input processed in 30-ms windows yielded very poor discriminative performance of movement phases (Fig. 3a;  $\bar{x}$  22%,  $+/-$  6.21, *specificity* = 37.9%, *sensitivity* = 51.9%). As expected, with extending the window duration to 150-ms, the phase classification improved ( $\bar{x}$  51%,  $+/-$  7.95, *specificity* = 49%, *sensitivity* = 52.8). However, contrary to the neural input, the global EMG did not allow for distinguishing between the same forces exerted during a decreasing and

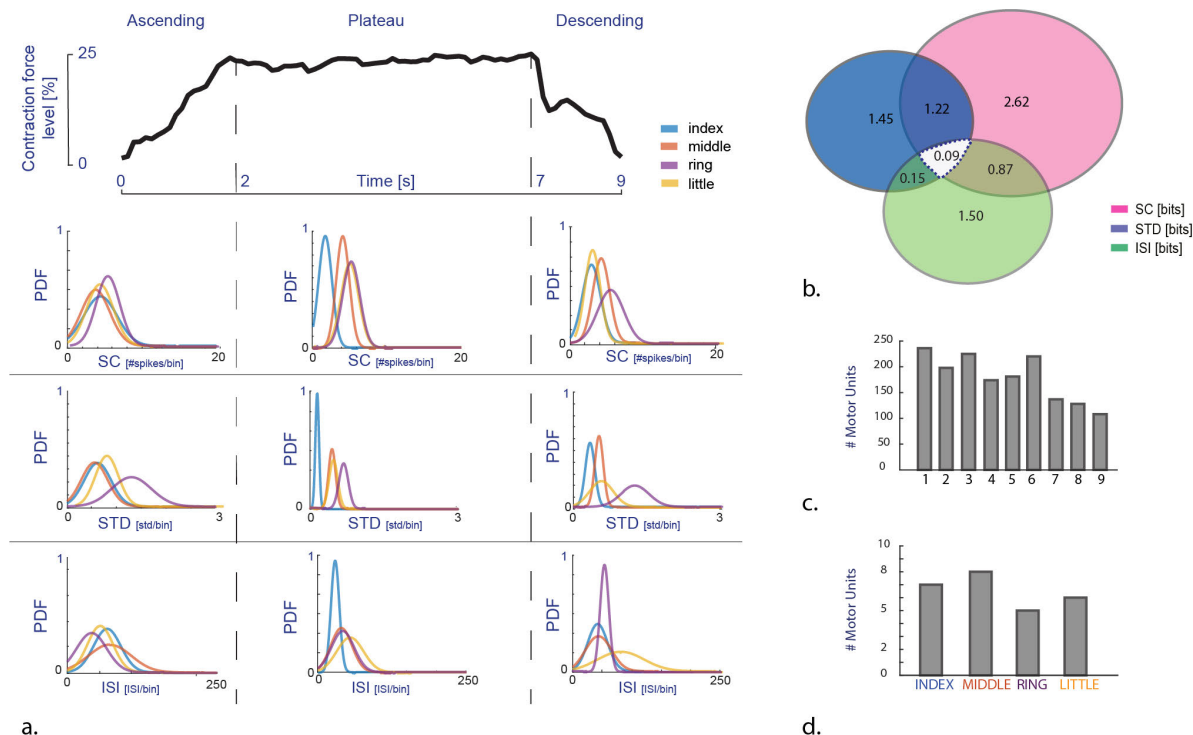


**FIGURE 2.** Feature space optimisation and motor unit quantitative analysis. **a.** Lower panel: the comparison of Poisson probability distribution of the extracted neural drive features (SC (spike count), STD (standard deviation), ISI (inter-spike interval)) for different finger flexions (color-coded) in movement phase context. The distribution plots for indicated intervals of 2s-5s-2s follow the force profile (upper panel) and correspond to the ascending (ASC), steady (PLAT) and descending (DESC) stages of a muscle contraction. Upper panel: exemplar finger flexion force profile sliced in intervals of 2s-5s-2s for the presentation purposes. Results in a. are based on a representative subject dataset. **b.** Mutual Information analysis for testing the feature set relevance averaged over all of the participants (Venn diagram presentation). Individual circles show the entropy corresponding to individual features, while the union of any two or three circles corresponds to the respective joint entropies. **c.** Number of motor units detected in all of the trials presented for all individual participants (1-9). **d.** Average number of motor units detected in different finger presses (index, middle, ring and little finger flexions) for all participants.

increasing muscle contraction regardless of the processing window size. The cause for a considerable difference in the classification accuracies between the neural and EMG inputs was the insufficient temporal resolution provided by the HD-EMG signal during transient phases of the contraction, explained in Fig. 3b. Therefore, the use of the decoded neural drive substantially expanded the identification of discriminative aspects of motor tasks with respect to the global EMG.

We next validated the possibility of tracking the muscle contraction stages while concurrently discriminating between different finger tasks. For this purpose, we classified individual DOFs (4) and their movement phases (3) (with muscle rest as an additional class, for a total of 13 classes). Fig. 4a shows the phase-and-DOF classification results for neural input averaged across all participants. The accuracy of the proposed neural approach in discriminating both individual finger movements and movement phases concurrently was very high (96.1%,  $\pm 0.061$ ), with a specificity of 98.3% and a sensitivity of 98.8%. For comparison, the global EMG failed to concurrently classify movement phases and DOF, as expected based on the poor accuracy when classifying only movement phases (results not shown). Our findings prove, for the first time, that a non-invasive interface with

muscles can provide a highly accurate recognition of volitional multi-DOF finger movements together with tracking all of the movements' phases with a delay smaller than any previously proposed HMI control system.

### B. RECOVERING FINGER CLASSES FROM CONTRACTION STAGES

Joint classification of DOF and movement phases allows for a highly accurate temporal identification of the activation and de-activation of an individual DOF, in a way that is robust to changes in force. To show the feasibility of accurate finger movement recognition when exerting variable forces, we computed the accuracy of DOF classification based on all movement phases. When using global EMG in variable force conditions, the classification error rate is high specifically when force varies around small values. Indeed, as it can be seen on the top of the Fig. 4b, an across-phase comparison proved that the DOF discrimination based on the global HD-EMG features processed in 150-ms windows was variable, with the accuracy highly reliant on the contraction stage used as an input to the classifier (total accuracy range (TAR): 43.6% for the descending phase input to 92% for the plateau phase input,  $\bar{x}$  71.25,  $\pm 20.19$ ). When using global

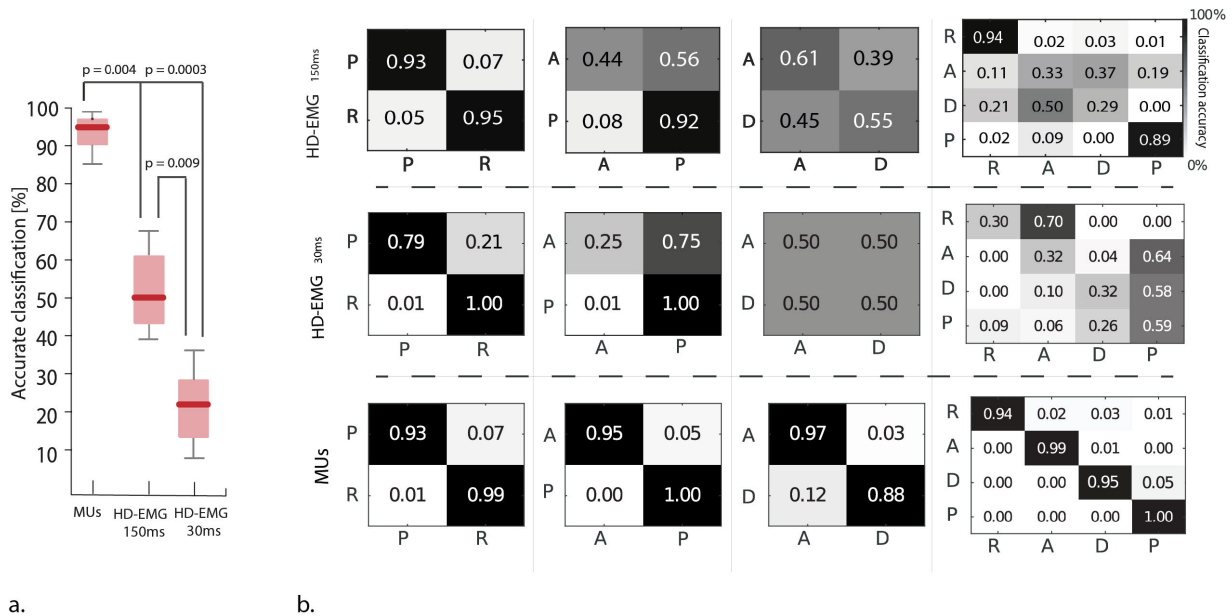


**FIGURE 3.** Contraction-phase classification results and classification progression for neural and global inputs. **a.** Classification accuracy output mean  $\pm$  s.d. for all of the subjects for neural and global inputs and varying processing window sizes. Data were compared using the independent samples t-test. **b.** Confusion matrices depicting classification accuracies for a representative subject and neural and global inputs for varying processing window sizes, after incremental addition of transient contraction information to the classification input. HD-EMG: global input, MUs: neural input. Contraction stages' classes: R – REST P – PLAT A – ASC D – DESC.

EMG on a much shorter processing interval of 30-ms the performance further decreased, as expected (results not shown). Conversely, the discrimination based on neural input features processed in 30-ms windows resulted in high accuracy regardless of the movement phase (TAR: 93% for the ascending phase input to 97.5% for the descending phase input,  $\bar{x}$  95,  $\pm$  2.73). On average, in the complete contraction context (condition labelled as MIX; full force range), the neural approach resulted in 98  $\pm$  0.3% DOF discrimination accuracy, and the global EMG resulted in 88  $\pm$  2.1% DOF discrimination accuracy while processed in 150-ms intervals ( $p = 0.04$ ) and 75%  $\pm$  3.7 while processed in 30-ms intervals. Therefore, the neural approach allowed a 10% more accurate DOF classification than the global EMG approach, when classification was performed on complete finger flexion data. Beside the average classification accuracy over all force, the difference in accuracy between the two classification inputs was as high as  $>50\%$  in the variable-force contraction stages, which are the most common stages in natural use of an HMI. These results are consistent with the findings presented in the previous section, and in agreement with previous research in showing that the global EMG properties are insufficient for an accurate DOF discrimination prior to reaching a steady contraction stage (see Discussion).

In summary, we showed for the first time that the recognition of individual fingers can be achieved with the accuracy of  $\sim 98\%$  for the full range of contraction forces investigated, and for an extremely short processing window (30-ms). This indicates that intended dexterous movements can be detected with a temporal resolution of 30-ms for any force exerted in an isometric contraction, with consistently very

high accuracy. The difference in performance with respect to global EMG (which showed  $<90\%$  accuracy on average and  $<50\%$  accuracy in specific task phases, for a much longer processing window of 150-ms) is substantial and shows a realistic potential for the proposed approach to be carried forward into large-scale user applications.

### C. GENERALISATION ACROSS INDIVIDUALS

Having demonstrated that the neural approach provides a successful multi-phase-and-DOF classification at all phases of the isometric muscle contraction, we then addressed the question whether the neural drive decoded with the EMG decomposition can be used as a universal movement code across humans without (or with minimal) user-specific training, and if so, how well does it generalise in comparison with the global EMG features. For this purpose, we classified different finger movements (4) and their contraction stages (3) based on a leave-one-out cross-validation model (LOOCV – see Methods) across subjects using neural and global EMG inputs.

First, we built the LOOCV (1) from a training set comprising the data of eight out of nine participants, with the test set comprising the 'left-out' participant's data. The results of our LOOCV (1) analysis, presented in the top row of Fig. 4c, show a large decrease in the classification accuracy on average when using the general model instead of the subject-specific model, for both types of the classification input ( $\bar{x}$  accuracy based on LOOCV(1): neural input = 40.33%  $\pm$  18.5, global EMG input = 6.84%,  $\pm$  3.1). As can be inferred from the muscle activation heat maps presented in the Appendix, Supplementary Fig. 3., the spatial

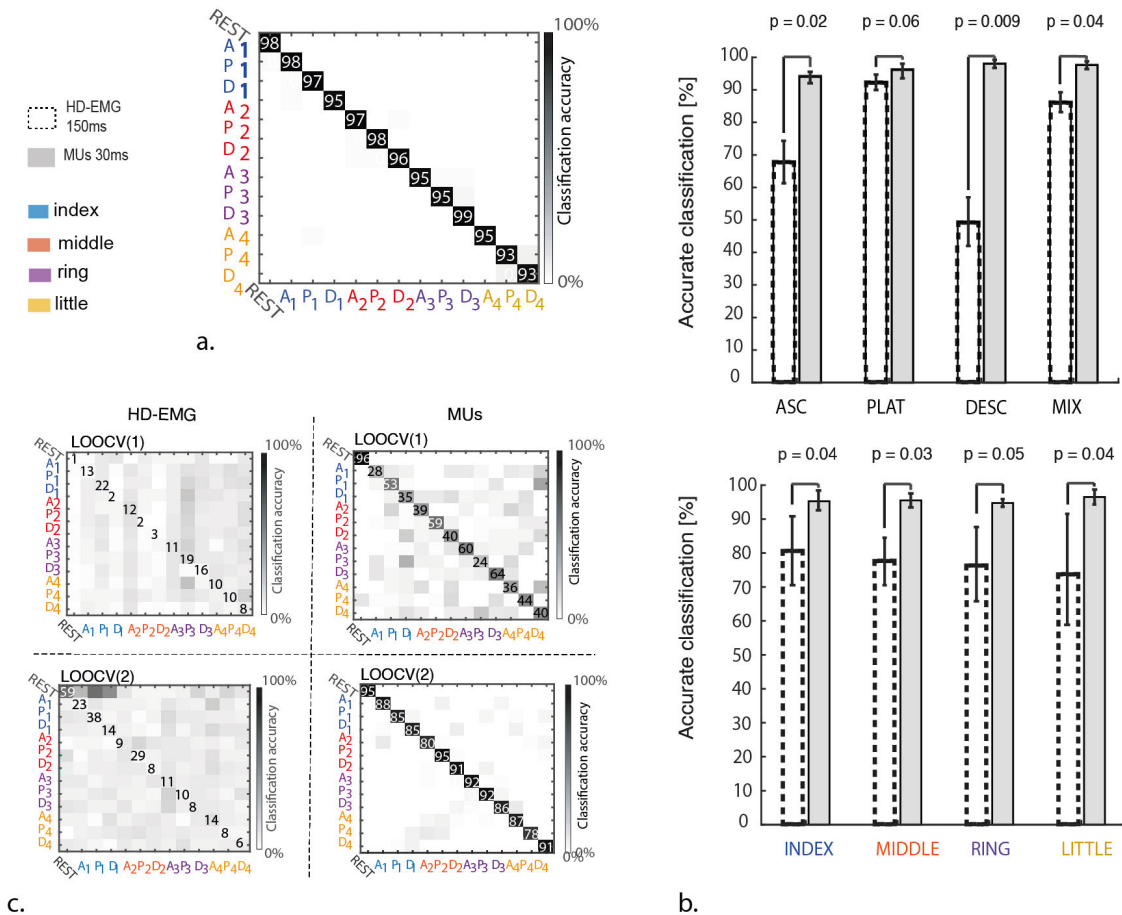


**FIGURE 4.** Average contraction-phase and DOF classification results for neural and global inputs with subject-specific and general discriminative variants. **a.** Confusion matrix depicting the average output of the neural-based, subject-specific contraction stages classification (averaging performed across all subjects). **b.** DOF classification accuracy output averages  $\pm$  s.ds. for neural and global inputs, for individual contraction stages and mixed (all) DOFs (top) and individual DOFs and mixed (all) phases (bottom) (averaging performed across all subjects). **c.** Confusion matrices depicting the average output of the EMG-based and MU-based contraction stages classification based on the general model (first row: LOOCV(1), second row: LOOCV(2)). A<sub>1</sub>, P<sub>1</sub>, D<sub>1</sub> – index finger contraction stages, A<sub>2</sub>, P<sub>2</sub>, D<sub>2</sub> – middle finger contraction stages, A<sub>3</sub>, P<sub>3</sub>, D<sub>3</sub> – ring finger contraction stages, A<sub>4</sub>, P<sub>4</sub>, D<sub>4</sub> – little finger contraction stages. Contraction stages’ classes: R – REST P – PLAT A – ASC D – DESC.

organisation of the muscle innervation detected from the skin level is the main limitation of the generalisation process, as it can differ significantly between people.

Next, we constructed the LOOCV (2) for which the training set comprised the LOOCV (1) training data with the addition of 5% of a left-out participant’s data (corresponding to just 6-s of recordings for each subject), and the test set the remaining 95% data from nine out of the ten participants. This testing condition corresponded to a universal interface based on a database of training data with the addition of a very small amount of user-specific training. As presented in Fig. 4c, the average accuracy of the inter-participant DOF-and-phase discrimination based on as little as 5% participant-specific neural information increased over two-fold with respect to the LOOCV(1) variant, and was only slightly lower than that of the average subject-specific classification showed in Fig. 4a ( $\bar{x}$  accuracy LOOCV(2): 90%,  $\pm$  0.38,  $\bar{x}$  accuracy – subject-specific training: 96.1%,  $\pm$  0.061, respectively). Conversely, the average LOOCV(2)-based

classification accuracy when using the EMG input remained very poor, as it was in the LOOCV(1) variant ( $\bar{x}$  accuracy LOOCV(2): 11.38%,  $\pm$  7.21). These findings imply that the peripheral neural information manifests universal properties across subjects. The small subject-specific information needed to exploit this generalisation across individuals relates to the effect of the subjects’ anatomy on the distribution of action potential amplitudes on the skin surface.

#### IV. DISCUSSION

We propose a technique for decoding an intended movement from the neural drive to the muscle. We observed that unlike the conventional peripheral movement decoding that uses global EMG signal features, our approach enabled a highly accurate, near-real time classification (30-ms data processing interval) of finger movements at any force level with successful movement phase discrimination. This result was obtained by using physiology-inspired neural drive features that displayed different statistical properties for both different

finger flexions and muscle contraction stages. Our pattern recognition of EMG signals and neural drive was complemented by an additional analysis of the universality of the peripheral neural information in humans, in which we discriminated the movements and their phases after excluding or limiting the amount of participant-specific information.

### A. EMG VS NEURAL DRIVE

Our study builds on previous work that applied non-invasive peripheral myoelectric analysis to study muscle activation patterns and movement control [20], [24], [40], [41]. Whereas the majority of the past studies used the indirect approach based on global features of the surface EMG to characterise a movement, we studied the neural information both indirectly with standard EMG signal analysis, and directly by decomposing HD-EMG signals into the neural drive to the muscles. Our results for individual finger movements when considering only a stable portion of force production are in agreement with recent findings reporting dexterous movement recognition from EMG signals [43]–[46], with the neural drive slightly outperforming the EMG input. While the gross EMG signal is sufficient for an accurate differentiation between movements at stable force level, the transient EMG (corresponding to ASC and DESC movement phases, or increase/decrease force levels) has non-stationary properties with variable mean and covariance [47], [48], making reliable pattern extraction difficult when contraction force varies. Nonetheless, control of HMIs is fundamentally based on variable-force contractions, causing difficulties for conventional EMG-based control systems. In agreement with previous research, we showed that the information carried in the global EMG features is insufficient for an accurate movement classification during the contraction onset and relaxation. This confirms that in order for the EMG-based intended movement decoding to be correct, it has to be delayed until a stable force level is achieved and halted right after [49]. While the problem of peripheral transient movement classification has been addressed in the past, the proposed solutions targeted transient decoding during the initial movement phase of force increase only [42], [50], provided validation for gross movement recognition but not dexterous [51], or validated the algorithms on a low amount of movements not exceeding 2 DOFs [52], [53]. Importantly, none of the previous studies achieved the performance we present here. Moreover, all previous studies focused on processing windows of hundreds of milliseconds. Our direct movement decoding method based on peripheral neural activity is highly advantageous in terms of the temporal structure and variability in comparison with the conventional surface EMG solutions. Together with the high-density electrode setup, our approach allows for establishing a movement analysis framework that offers a superior spatio-temporal resolution of muscle activity that accompanies movement execution. In the context of daily living, the direct neural decoding can significantly enhance the HMI systems' robustness. Providing an extremely high classification accuracy of >98%, based on near-real time

30-ms processing intervals, it allows for an accurate intended actuation of different DOFs with a minimal delay accompanying the movement class switching.

### B. DECODING AND TRACKING INTENDED MOVEMENT WITH PERIPHERAL NEURAL CORRELATES

The ultimate neural determinant of motion is the firing of spinal motor neurons that excites the contractile tissue [30], [54]. Thus, at the peripheral level, muscles and (by proxy) movements are controlled by the motor neurons' timings of action potentials discharges. This neural information has been successfully used for classifying gross grasps and wrist movements [21], [27], [28]. Here, we designed a set of features extracted from motor neuron activation timings that represents the temporal structure of motor neuron activation. The force exerted by a muscle during a voluntary contraction depends on the number of active motor units (i.e. motor unit recruitment), and the rates at which the motor neurons discharge action potentials (i.e. rate coding) [30], [31]. Concurrent changes in these two properties control the force generated by the muscle: an increase (decrease) in force follows the increase (decrease) in motor unit recruitment and motor neuron firing rate. Recruitment is difficult to track accurately by EMG decomposition since the decomposition does not identify all active motor units but only a subset [32]. For this reason, our quantitative motor unit analysis showed that a similar number of units was identified across different finger flexion tasks (Fig. 2c-d, Appendix, Supplementary Fig. 1.). On the other hand, rate coding can be detected with good temporal resolution even from a small subset of identified motor units. The features we proposed for characterising the neural drive reflect both mechanisms. The first extracted feature was the sum of spikes, which is an estimate of the strength of the neural drive to the muscle based on the subset of identified units. This feature is proportional to the force exerted by the muscle [47], and therefore contains information for discriminating steady (PLAT) movement phases from transient (ASC, DESC). The second feature was the standard deviation of the timings, which measures the temporal spread of the detected action potentials in the processing window. This feature proved helpful in discriminating between different contraction stages and DOFs in cases when the sum of spikes was equal for different conditions. As for the third and final feature, we extracted the mean inter-spike interval in order to determine whether spikes were fired in bursts or continuously. Recruitment information was mainly associated to the spatial distribution of the detected motor unit action potentials in different finger flexion tasks, thus it was addressed with the spatial activation thresholding of the feature space. Physiological information embedded in the selected feature space could not be obtained from the global EMG, which explains the large difference in performance between the proposed method and conventional EMG classification, especially for challenging classification tasks (such as for the same force during and increasing or decreasing trend).

### C. TESTING THE UNIVERSALITY OF PERIPHERAL NEURAL INFORMATION AMONG HUMANS

Understanding the neural principles underlying the generation of a voluntary action remains a major neuroscientific goal [55]. Towards this end, we identified a set of physiology-inspired spatio-temporal properties of motor neuron activity that, collectively, explained force generation during various isometric dexterous contractions. Because motor unit recruitment and rate coding accompany muscle activation across all humans [30], [48], we hypothesized that the proposed neural feature set, which is based on these two mechanisms, would generalize across participants. The relatively accurate movement discrimination achieved with the leave-one-subject-out cross validation using a linear classification algorithm indicated that the selected features are associated to movement in a similar way across the investigated subjects; yet, we observed a decrease in performance with respect to subject-specific training. We infer that this was due to our feature space comprising the information related to the spatial distribution of action potential amplitudes, which is influenced by the volume conductor properties and therefore by the participant's anatomy. Eliminating this feature may increase the generality of the model across individuals, however the discriminative power of our approach would decrease since motor unit recruitment cannot be easily tracked with only temporal features. Interestingly, we found that by training the classifier on a small amount of participant-specific data, we achieved classification accuracy close to the ideal case of subject-specific training. In the context of neural interfacing, this finding implies that the extensive training periods usually required for an accurate calibration of HMIs [56], [57] can undergo significant reduction, shifting the paradigm towards more effective and user-friendly systems.

### REFERENCES

- [1] D. M. Wolpert and Z. Ghahramani, "Computational principles of movement neuroscience," *Nature Neurosci.*, vol. 3, no. S11, pp. 1212–1217, Nov. 2000, doi: [10.1038/81497](https://doi.org/10.1038/81497).
- [2] E. Todorov, "Direct cortical control of muscle activation in voluntary arm movements: A model," *Nature Neurosci.*, vol. 3, no. 4, pp. 391–398, Apr. 2000, doi: [10.1038/73964](https://doi.org/10.1038/73964).
- [3] H. Kim, N. Yoshimura, and Y. Koike, "Classification of movement intention using independent components of premovement EEG," *Frontiers Hum. Neurosci.*, vol. 13, p. 63, Feb. 2019, doi: [10.3389/fnhum.2019.00063](https://doi.org/10.3389/fnhum.2019.00063).
- [4] B. K. Kang, J. S. Kim, S. Ryun, and C. K. Chung, "Prediction of movement intention using connectivity within motor-related network: An electrocorticography study," *PLoS ONE*, vol. 13, no. 1, Jan. 2018, Art. no. e0191480, doi: [10.1371/journal.pone.0191480](https://doi.org/10.1371/journal.pone.0191480).
- [5] J.-N. Kim and M. N. Shadlen, "Neural correlates of a decision in the dorsolateral prefrontal cortex of the macaque," *Nature Neurosci.*, vol. 2, no. 2, pp. 176–185, Feb. 1999, doi: [10.1038/5739](https://doi.org/10.1038/5739).
- [6] J. D. Schall, "Neural basis of deciding, choosing and acting," *Nature Rev. Neurosci.*, vol. 2, no. 1, pp. 33–42, Jan. 2001, doi: [10.1038/35049054](https://doi.org/10.1038/35049054).
- [7] M. D. Serruya, N. G. Hatsopoulos, L. Paninski, M. R. Fellous, and J. P. Donoghue, "Instant neural control of a movement signal," *Nature*, vol. 416, no. 6877, pp. 141–142, Mar. 2002, doi: [10.1038/416141a](https://doi.org/10.1038/416141a).
- [8] J. Pereira, P. Ofner, A. Schwarz, A. I. Sburlea, and G. R. Müller-Putz, "EEG neural correlates of goal-directed movement intention," *NeuroImage*, vol. 149, pp. 129–140, Apr. 2017, doi: [10.1016/j.neuroimage.2017.01.030](https://doi.org/10.1016/j.neuroimage.2017.01.030).
- [9] W. Stadler, A. Springer, J. Parkinson, and W. Prinz, "Movement kinematics affect action prediction: Comparing human to non-human point-light actions," *Psychol. Res.*, vol. 76, no. 4, pp. 395–406, Jul. 2012, doi: [10.1007/s00426-012-0431-2](https://doi.org/10.1007/s00426-012-0431-2).
- [10] M. Baglioni, J. A. Fernandes de Macêdo, C. Renso, R. Trasarti, and M. Wachowicz, *Towards Semantic Interpretation of Movement Behavior*. Berlin, Germany: Springer, 2009, pp. 271–288.
- [11] A. E. Olsson, P. Sager, E. Andersson, A. Björkman, N. Malešević, and C. Antfolk, "Extraction of multi-labelled movement information from the raw HD-sEMG image with time-domain depth," *Sci. Rep.*, vol. 9, no. 1, pp. 1–10, Dec. 2019, doi: [10.1038/s41598-019-43676-8](https://doi.org/10.1038/s41598-019-43676-8).
- [12] E. Trigili, L. Grazi, S. Crea, A. Accogli, J. Carpaneto, S. Micera, N. Vitiello, and A. Panarese, "Detection of movement onset using EMG signals for upper-limb exoskeletons in reaching tasks," *J. Neuroeng. Rehabil.*, vol. 16, no. 1, pp. 1–16, Mar. 2019, doi: [10.1186/s12984-019-0512-1](https://doi.org/10.1186/s12984-019-0512-1).
- [13] S. Dosen, M. Markovic, K. Somer, B. Graimann, and D. Farina, "EMG biofeedback for online predictive control of grasping force in a myoelectric prosthesis," *J. Neuroeng. Rehabil.*, vol. 12, no. 1, pp. 1–13, Jun. 2015, doi: [10.1186/s12984-015-0047-z](https://doi.org/10.1186/s12984-015-0047-z).
- [14] U. Chaudhary, N. Birbaumer, and A. Ramos-Murguialday, "Brain-computer interfaces for communication and rehabilitation," *Nature Rev. Neurol.*, vol. 12, pp. 513–525, Aug. 2016, doi: [10.1038/nrneurol.2016.113](https://doi.org/10.1038/nrneurol.2016.113).
- [15] S. L. Norman, M. Dennison, E. Wolbrecht, S. C. Cramer, R. Srinivasan, and D. J. Reinkensmeyer, "Movement anticipation and EEG: Implications for BCI-contingent robot therapy," *IEEE Trans. Neural Syst. Rehabil. Eng.*, vol. 24, no. 8, pp. 911–919, Aug. 2016, doi: [10.1109/TNSRE.2016.2528167](https://doi.org/10.1109/TNSRE.2016.2528167).
- [16] D. Farina and O. Aszmann, "Bionic limbs: Clinical reality and academic promises," *Sci. Transl. Med.*, vol. 6, pp. 257–1–257-12, Oct. 2014, doi: [10.1126/scitranslmed.3010453](https://doi.org/10.1126/scitranslmed.3010453).
- [17] J. L. Contreras-Vidal, J. Cruz-Garcia, and A. Kopteva, "Towards a whole body brain-machine interface system for decoding expressive movement intent challenges and opportunities," in *Proc. 5th Int. Winter Conf. Brain-Comput. Interface (BCI)*, Jan. 2017, pp. 1–4, doi: [10.1109/IWW-BCI.2017.7858142](https://doi.org/10.1109/IWW-BCI.2017.7858142).
- [18] R. A. Ramadan and A. V. Vasilakos, "Brain computer interface: Control signals review," *Neurocomputing*, vol. 223, pp. 26–44, Feb. 2017.
- [19] I. Lazarou, S. Nikolopoulos, P. C. Petrantonakis, I. Kompatsiaris, and M. Tsolaki, "EEG-based brain-computer interfaces for communication and rehabilitation of people with motor impairment: A novel approach of the 21st century," *Frontiers Hum. Neurosci.*, vol. 12, p. 14, Jan. 2018, doi: [10.3389/fnhum.2018.00014](https://doi.org/10.3389/fnhum.2018.00014).
- [20] J. B. Nielsen, "Human spinal motor control," *Annu. Rev. Neurosci.*, vol. 39, no. 1, pp. 81–101, Jul. 2016, doi: [10.1146/annurev-neuro-070815-013913](https://doi.org/10.1146/annurev-neuro-070815-013913).
- [21] D. Farina, I. Vujaklija, M. Sartori, T. Kapelner, F. Negro, N. Jiang, K. Bergmeister, A. Andali, J. Principe, and O. C. Aszmann, "Man/machine interface based on the discharge timings of spinal motor neurons after targeted muscle reinnervation," *Nature Biomed. Eng.*, vol. 1, no. 2, pp. 1–12, Feb. 2017, doi: [10.1038/s41551-016-0025](https://doi.org/10.1038/s41551-016-0025).
- [22] D. Farina, F. Negro, M. Gazzoni, and R. M. Enoka, "Detecting the unique representation of motor-unit action potentials in the surface electromyogram," *J. Neurophysiol.*, vol. 100, no. 3, pp. 1223–1233, Sep. 2008, doi: [10.1152/jn.90219.2008](https://doi.org/10.1152/jn.90219.2008).
- [23] D. Staudenmann, I. Kingma, A. Daffertshofer, D. F. Stegeman, and J. H. van Dieën, "Improving EMG-based muscle force estimation by using a high-density EMG grid and principal component analysis," *IEEE Trans. Biomed. Eng.*, vol. 53, no. 4, pp. 712–719, Apr. 2006, doi: [10.1109/TBME.2006.870246](https://doi.org/10.1109/TBME.2006.870246).
- [24] D. Farina, A. Holobar, R. Merletti, and R. M. Enoka, "Decoding the neural drive to muscles from the surface electromyogram," *Clin. Neurophysiol.*, vol. 121, no. 10, pp. 1616–1623, Oct. 2010, doi: [10.1016/j.clinph.2009.10.040](https://doi.org/10.1016/j.clinph.2009.10.040).
- [25] D. Farina and F. Negro, "Accessing the neural drive to muscle and translation to neurorehabilitation technologies," *IEEE Rev. Biomed. Eng.*, vol. 5, pp. 3–14, 2012, doi: [10.1109/RBME.2012.2183586](https://doi.org/10.1109/RBME.2012.2183586).
- [26] D. Y. Barsakcioglu and D. Farina, "A real-time surface EMG decomposition system for non-invasive human-machine interfaces," in *Proc. IEEE Biomed. Circuits Syst. Conf. (BioCAS)*, Oct. 2018, pp. 1–4, doi: [10.1109/BIOCAS.2018.8584659](https://doi.org/10.1109/BIOCAS.2018.8584659).
- [27] T. Kapelner, I. Vujaklija, N. Jiang, F. Negro, O. C. Aszmann, J. Principe, and D. Farina, "Predicting wrist kinematics from motor unit discharge timings for the control of active prostheses," *J. Neuroeng. Rehabil.*, vol. 16, no. 1, Dec. 2019.

- [28] C. Chen, Y. Yu, S. Ma, X. Sheng, C. Lin, D. Farina, and X. Zhu, "Hand gesture recognition based on motor unit spike trains decoded from high-density electromyography," *Biomed. Signal Process. Control*, vol. 55, Jan. 2020, Art. no. 101637, doi: [10.1016/j.bspc.2019.101637](https://doi.org/10.1016/j.bspc.2019.101637).
- [29] T. Kapelner, N. Jiang, A. Holobar, I. Vujaklija, A. D. Roche, D. Farina, and O. C. Aszmann, "Motor unit characteristics after targeted muscle reinnervation," *PLoS ONE*, vol. 11, no. 2, Feb. 2016, Art. no. e0149772, doi: [10.1371/journal.pone.0149772](https://doi.org/10.1371/journal.pone.0149772).
- [30] R. M. Enoka and J. Duchateau, "Rate coding and the control of muscle force," *Cold Spring Harbor Perspect. Med.*, vol. 7, no. 10, Oct. 2017, Art. no. a029702, doi: [10.1101/cshperspect.a029702](https://doi.org/10.1101/cshperspect.a029702).
- [31] K. Saitou, T. Masuda, D. Michikami, R. Kojima, and M. Okada, "Innervation zones of the upper and lower limb muscles estimated by using multichannel surface EMG," *J. Hum. Ergol.*, vol. 29, nos. 1–2, pp. 35–52, Dec. 2000, doi: [10.11183/jhe1972.29.35](https://doi.org/10.11183/jhe1972.29.35).
- [32] A. Holobar, D. Farina, M. Gazzoni, R. Merletti, and D. Zazula, "Estimating motor unit discharge patterns from high-density surface electromyogram," *Clin. Neurophysiol.*, vol. 120, no. 3, pp. 551–562, Mar. 2009, doi: [10.1016/j.clinph.2008.10.160](https://doi.org/10.1016/j.clinph.2008.10.160).
- [33] J. D. Victor, "Spike train metrics," *Current Opinion Neurobiol.*, vol. 15, no. 5, pp. 585–592, Oct. 2005, doi: [10.1016/j.conb.2005.08.002](https://doi.org/10.1016/j.conb.2005.08.002).
- [34] J. R. Vergara and P. A. Estévez, "A review of feature selection methods based on mutual information," *Neural Comput. Appl.*, vol. 24, no. 1, pp. 175–186, Jan. 2014.
- [35] K. S. Kim, H. H. Choi, C. S. Moon, and C. W. Mun, "Comparison of k-nearest neighbor, quadratic discriminant and linear discriminant analysis in classification of electromyogram signals based on the wrist-motion directions," *Current Appl. Phys.*, vol. 11, no. 3, pp. 740–745, May 2011, doi: [10.1016/j.cap.2010.11.051](https://doi.org/10.1016/j.cap.2010.11.051).
- [36] J. Shao, "Linear model selection by cross-validation," *J. Amer. Stat. Assoc.*, vol. 88, no. 422, pp. 486–494, Jun. 1993, doi: [10.1080/01621459.1993.10476299](https://doi.org/10.1080/01621459.1993.10476299).
- [37] M. Stone, "Cross-validated choice and assessment of statistical predictions," *J. Roy. Stat. Soc., B (Methodol.)*, vol. 36, no. 2, pp. 111–133, Jan. 1974, doi: [10.1111/j.2517-6161.1974.tb00994.x](https://doi.org/10.1111/j.2517-6161.1974.tb00994.x).
- [38] R. Kohavi, "A study of cross-validation and bootstrap for accuracy estimation and model selection," *Ijcai*, vol. 14, no. 2, pp. 1137–1145, Aug. 1995.
- [39] S. Tabe-Bordbar, A. Emad, S. D. Zhao, and S. Sinha, "A closer look at cross-validation for assessing the accuracy of gene regulatory networks and models," *Sci. Rep.*, vol. 8, no. 1, pp. 1–11, Dec. 2018, doi: [10.1038/s41598-018-24937-4](https://doi.org/10.1038/s41598-018-24937-4).
- [40] L. A. Kallenberg and H. J. Hermens, "Behaviour of motor unit action potential rate, estimated from surface EMG, as a measure of muscle activation level," *J. Neuroeng. Rehabil.*, vol. 3, no. 1, pp. 1–13, Jul. 2006, doi: [10.1186/1743-0003-3-15](https://doi.org/10.1186/1743-0003-3-15).
- [41] M. Gazzoni, A. Botter, and T. Vieira, "Surface EMG for human-machine interfaces: New knowledge and open issues," in *Mech. Mach. Sci.*, vol. 49, pp. 911–918, 2018, doi: [10.1007/978-3-319-61276-8\\_97](https://doi.org/10.1007/978-3-319-61276-8_97).
- [42] G. Kanitz, C. Cipriani, and B. B. Edin, "Classification of transient myoelectric signals for the control of multi-grasp hand prostheses," *IEEE Trans. Neural Syst. Rehabil. Eng.*, vol. 26, no. 9, pp. 1756–1764, Sep. 2018, doi: [10.1109/TNSRE.2018.2861465](https://doi.org/10.1109/TNSRE.2018.2861465).
- [43] N. Celadon, S. Došen, I. Binder, P. Ariano, and D. Farina, "Proportional estimation of finger movements from high-density surface electromyography," *J. Neuroeng. Rehabil.*, vol. 13, no. 1, pp. 1–19, Aug. 2016, doi: [10.1186/s12984-016-0172-3](https://doi.org/10.1186/s12984-016-0172-3).
- [44] F. V. G. Tenore, A. Ramos, A. Fahmy, S. Acharya, R. Etienne-Cummings, and N. V. Thakor, "Decoding of individuated finger movements using surface electromyography," *IEEE Trans. Biomed. Eng.*, vol. 56, no. 5, pp. 1427–1434, May 2009, doi: [10.1109/TBME.2008.2005485](https://doi.org/10.1109/TBME.2008.2005485).
- [45] Y. Na, S. J. Kim, S. Jo, and J. Kim, "Ranking hand movements for myoelectric pattern recognition considering forearm muscle structure," *Med. Biol. Eng. Comput.*, vol. 55, no. 8, pp. 1507–1518, Aug. 2017, doi: [10.1007/s11517-016-1608-4](https://doi.org/10.1007/s11517-016-1608-4).
- [46] A. H. Al-Timemy, G. Bugmann, J. Escudero, and N. Outram, "Classification of finger movements for the dexterous hand prosthesis control with surface electromyography," *IEEE J. Biomed. Health Informat.*, vol. 17, no. 3, pp. 608–618, May 2013, doi: [10.1109/JBHI.2013.2249590](https://doi.org/10.1109/JBHI.2013.2249590).
- [47] A. M. Taylor, E. A. Christou, and R. M. Enoka, "Multiple features of motor-unit activity influence force fluctuations during isometric contractions," *J. Neurophysiol.*, vol. 90, no. 2, pp. 1350–1361, Aug. 2003, doi: [10.1152/jn.00056.2003](https://doi.org/10.1152/jn.00056.2003).
- [48] C. J. De Luca, "Control properties of motor units," *J. Exp. Biol.*, vol. 115, no. 1, pp. 125–136, 1985.
- [49] A. J. Fuglevand, D. A. Winter, and A. E. Patla, "Models of recruitment and rate coding organization in motor-unit pools," *J. Neurophysiol.*, vol. 70, no. 6, pp. 2470–2488, Dec. 1993, doi: [10.1152/jn.1993.70.6.2470](https://doi.org/10.1152/jn.1993.70.6.2470).
- [50] B. Hudgins, P. Parker, and R. N. Scott, "A new strategy for multifunction myoelectric control," *IEEE Trans. Biomed. Eng.*, vol. 40, no. 1, pp. 82–94, Jan. 1993, doi: [10.1109/10.204774](https://doi.org/10.1109/10.204774).
- [51] D. Yang, J. Zhao, L. Jiang, and H. Liu, "Dynamic hand motion recognition based on transient and steady-state EMG signals," *Int. J. Humanoid Robot.*, vol. 09, no. 01, Mar. 2012, Art. no. 1250007, doi: [10.1142/S0219843612500077](https://doi.org/10.1142/S0219843612500077).
- [52] N. Jiang, T. Lorrain, and D. Farina, "A state-based, proportional myoelectric control method: Online validation and comparison with the clinical state-of-the-art," *J. Neuroeng. Rehabil.*, vol. 11, no. 1, p. 110, 2014, doi: [10.1186/1743-0003-11-110](https://doi.org/10.1186/1743-0003-11-110).
- [53] M. P. Mobarak, R. M. Guerrero, J. M. G. Salgado, and V. L. Dorr, "Hand movement classification using transient state analysis of surface multichannel EMG signal," in *Proc. Pan Amer. Health Care Exchanges (PAHCE)*, Apr. 2014, pp. 1–6, doi: [10.1109/PAHCE.2014.6849622](https://doi.org/10.1109/PAHCE.2014.6849622).
- [54] C. J. De Luca, A. Adam, R. Wotiz, L. D. Gilmore, and S. H. Nawab, "Decomposition of surface EMG signals," *J. Neurophysiol.*, vol. 96, no. 3, pp. 1646–1657, Sep. 2006, doi: [10.1152/jn.00009.2006](https://doi.org/10.1152/jn.00009.2006).
- [55] R. Porter and R. Lemon, *Corticospinal Function and Voluntary Movement*, vol. 45. New York, NY, USA: Oxford Univ. Press, 1993.
- [56] T. Kapelner, M. Sartori, F. Negro, and D. Farina, "Neuro-musculoskeletal mapping for man-machine interfacing," *Sci. Rep.*, vol. 10, no. 1, pp. 1–10, Dec. 2020, doi: [10.1038/s41598-020-62773-7](https://doi.org/10.1038/s41598-020-62773-7).
- [57] J. M. Carmena, "Advances in neuroprosthetic learning and control," *PLoS Biol.*, vol. 11, no. 5, May 2013, Art. no. e1001561, doi: [10.1371/journal.pbio.1001561](https://doi.org/10.1371/journal.pbio.1001561).



**MARTYNA STACHACZYK** (Graduate Student Member, IEEE) received the B.Sc. degree in neuroscience from Jagiellonian University, Poland, in 2016, and the M.Res. degree in neurotechnology from Imperial College London, U.K., in 2017, where she is currently pursuing the Ph.D. degree with the Department of Bioengineering, under the supervision of Prof. Dario Farina.

Her research interests include neural signal processing, bio-inspired algorithms development, and information theoretical analysis of neural data. She received the EPSRC Studentship Award from Imperial College London.



**S. FAROKH ATASHZAR** (Member, IEEE) is currently an Assistant Professor of electrical and computer engineering, as well as mechanical and aerospace engineering with New York University (NYU). He is also with NYU Wireless. He leads the Medical Robotics and Interactive Intelligent Technologies (MERIT) Laboratory, NYU. He was ranked among the top five applicants in Canada for 2018 Natural Sciences and Engineering Research Council (NSERC) Postdoctoral Fellowship competition in the Electrical and Computer Engineering Sector.

His research interest includes human-robot interaction and integration. Before joining NYU, he was a Postdoctoral Scientist with the Department of Bioengineering, Imperial College London, U.K.



**SIGRID DUPAN** (Member, IEEE) received the M.Eng. degree in architecture from Ghent University, Belgium, in 2010, the M.Sc. degree in bio-engineering from Trinity College Dublin, Ireland, in 2014, and the Ph.D. degree from Radboud University Nijmegen, The Netherlands, in 2018, where she was a Marie Curie ECR. She was a Visiting Ph.D. Student with the University of Western Ontario, Canada, in 2016. She was a Visiting Ph.D. Student with Goettingen University, Germany, in 2017. From 2017 to 2018, she was a Visiting Ph.D. Student with Imperial College London, U.K. She is currently a Postdoctoral Researcher with the Intelligent Sensing Laboratory, School of Engineering, Newcastle University, U.K. Her research interests include closed-loop prosthetic control, understanding the underlying neural correlates of hand movements, and how sensory feedback can help prosthetic users.



**IVAN VUJAKLIJA** (Member, IEEE) received the degree in electrical engineering and computer science from the University of Belgrade, the M.Sc. degree in biomedical engineering from the University of Lübeck, and the Ph.D. degree in human medical sciences from the University of Göttingen, in 2016. He was working as a Research Assistant with the University Medical Center Göttingen, Institute of Neurorehabilitation Systems, Georg-August University. From 2012 to 2014, he worked with Ottobock Healthcare GmbH, Duderstadt, one of the world-leading prosthetic manufacturers. He was a Research Fellow with Arizona State University and Medical University of Vienna, in 2014 and 2015, respectively. From 2017 to 2018, he was a Research Associate with the Department of Bioengineering, Imperial College London. He is currently an Assistant Professor with the Department of Electrical Engineering and Automation, Aalto University, where he is the Head of the Bionic and Rehabilitation Engineering Research Group. He was a part of a team of researchers that pioneered techniques for non-invasive spinal interfacing for rehabilitation applications. The same team has successfully introduced a novel, technology driven surgical paradigm for limb reconstruction which is now becoming a clinical state of the art. His research interests include bio-signal processing, advanced control algorithms, prosthetics, robotics, translational neurorehabilitation, and neural control of movement.



**DARIO FARINA** (Fellow, IEEE) was a Full Professor with Aalborg University and the University Medical Center Göttingen, Georg-August University, where he founded and directed the Department of Neurorehabilitation Systems, acting as the Chair in Neuroinformatics of the Bernstein Focus Neurotechnology Göttingen. He is currently a Full Professor and a Chair in neurorehabilitation engineering with the Department of Bioengineering, Imperial College London. His research interests include biomedical signal processing, neurorehabilitation technology, and neural control of movement. He has been elected Fellow of AIMBE, ISEK, and EAMBES. He was a recipient of the 2010 IEEE Engineering in Medicine and Biology Society Early Career Achievement Award and the Royal Society Wolfson Research Merit Award. He has been the President of the International Society of Electrophysiology and Kinesiology (ISEK). He is also the Editor-in-Chief of the official Journal of this Society, the *Journal of Electromyography and Kinesiology*. He is also an Editor of *Science Advances*, the IEEE TRANSACTIONS ON BIOMEDICAL ENGINEERING, the IEEE TRANSACTIONS ON MEDICAL ROBOTICS AND BIONICS, *Wearable Technologies*, and the *Journal of Physiology*.

...